

A direct quantitative relationship between the functional properties of human and macaque V5

Geraint Rees^{1,2}, Karl Friston² and Christof Koch¹

¹ Division of Biology 139-74, California Institute of Technology, Pasadena, California 91125, USA

² Wellcome Department of Cognitive Neurology, Institute of Neurology, University College London, 12 Queen Square, London WC1N 3BG, UK

Correspondence should be addressed to G.R. (geraint@klab.caltech.edu)

The nature of the quantitative relationship between single-neuron recordings in monkeys and functional magnetic resonance imaging (fMRI) measurements in humans is crucial to understanding how experiments in these different species are related, yet it remains undetermined. We measured brain activity in humans attending to moving visual stimuli, using blood oxygenation level-dependent (BOLD) fMRI. Responses in V5 showed a strong and highly linear dependence on increasing strength of motion signal (coherence). These population responses in human V5 had a remarkably simple mathematical relationship to previously observed single-cell responses in macaque V5. We provided an explicit quantitative estimate for the interspecies comparison of single-neuron activity and BOLD population responses. Our data show previously unknown dissociations between the functional properties of human V5 and other human motion-sensitive areas, thus predicting similar dissociations for the properties of single neurons in homologous areas of macaque cortex.

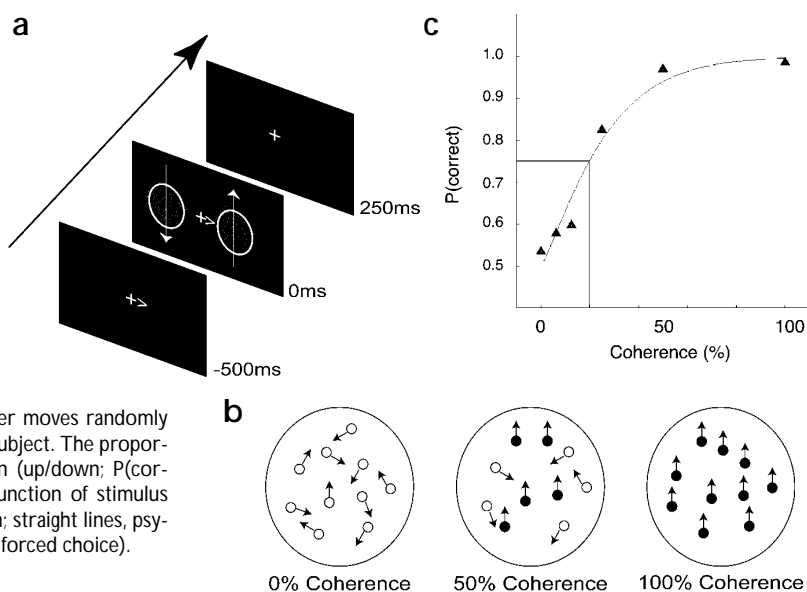
Understanding the relationship between brain activity and motion perception in the human visual system requires appreciation of not only which visual areas participate in motion processing, but also how their responses vary with visual characteristics of the stimulus. Much of our current knowledge of physiological responses underlying human motion perception has been inferred from detailed studies of single-neuron response properties in area V5/MT of the monkey^{1,2}. For example, responses of area V5 in macaque monkeys to dynamic random dot stimuli during a motion discrimination task³ show that individual V5 neurons carry directional signals of sufficient precision to account for psychophysical sensitivity to motion⁴. Furthermore, ablation of V5 impairs task performance⁵, electrical microstimulation of V5 influences choices in direction discrimination tasks⁶, and individual V5 neurons show monotonically increasing responses to stimulus coherence⁷. Taken together, these findings suggest that directional signals in macaque V5 contribute directly to the perception of motion.

Human motion perception has recently been studied using fMRI^{8,9}. The most commonly used fMRI contrast mechanism, BOLD contrast, measures changes in the local concentration of deoxyhemoglobin, providing an indirect but non-invasive index of local neuronal activity¹⁰. In humans, the best resolution now available with this technique is around one cortical column, which contains some 10^5 neurons. In the macaque monkey, state-of-the-art techniques have pushed the resolution down to smaller volumes of cortex, still comprising some $125 \mu\text{m}^3$ (ref. 11). Thus, fMRI in both species measures the responses of large populations of neurons, rather than single cells. The relationship between these two measures of cortical activity is poorly understood, yet is critical to understanding

the implications of experiments in non-human primates for human motion perception. Although this relationship is often assumed to be straightforward, computational simulation of neuronal populations in area V5 shows a complex relationship between activity in single cells and neuronal populations. In particular, simulated population responses to a stimulus may remain unchanged, despite large variation in the activity of single neurons¹². A quantitative appreciation of the relationship between single-neuron activity and population responses measured using fMRI remains elusive. One innovative recent experiment showed that an opponent motion stimulus elicits similar aggregate multi-neuron responses in macaque V5 and BOLD contrast responses in human V5 (ref. 13). However, this comparison was qualitative rather than quantitative, and focused on aggregate electrical activity rather than single-neuron recordings.

Understanding the relationship between single-neuron recordings and fMRI measurements is further complicated by differences in experimental protocols. In electrophysiology, it is usual to characterize single-neuron responses to extensive parametric variation of an experimental variable of interest (such as the strength of motion signal). However most human imaging studies compare only a single pair of experimental conditions (for example, the presence and absence of visual motion). Although such categorical comparisons can provide useful information about the location of human brain areas responsive to motion stimuli, they are of only limited utility in studying the computational mechanisms underlying motion stimuli¹⁴. We therefore sought to characterize in detail the cortical responses of human V5 to parametric variation in the strength of motion signal, and to analytically relate these responses to existing data from single neurons in macaque V5.

Fig. 1. Experimental paradigm and behavioral results. (a) Stimulus configuration. Each trial began with presentation of a cue (not drawn to scale) that indicated which aperture subjects attended. Then, 500 ms later, stochastic motion displays (Methods) were presented for 250 ms in each aperture. Stimulus coherence was identical in each aperture but direction of motion (vertical arrows here; not present in actual displays) was randomized independently between apertures. (b) Stimulus schemata for three different levels of coherence. At 0% coherence, all dots move in a random manner on successive frames. At 100% coherence, all dots move in a fully coherent fashion in one direction. For intermediate levels of coherence, the dots fall into two populations: one moves coherently (black symbols) and the other moves randomly (white symbols). (c) Psychophysical results for one subject. The proportion of correct judgements for direction of motion (up/down; $P(\text{correct})$) in the reported aperture are plotted as a function of stimulus coherence. Curved line, best-fitting Weibull function; straight lines, psychophysical threshold (75% correct, two-alternative forced choice).



RESULTS

Brief presentations of dynamic random dot stimuli were used to evaluate human brain responses to different strengths of motion signal (coherence) using BOLD contrast fMRI. For each trial, patches of coherently moving dots were presented either side of fixation (Methods and Fig. 1a). Each patch moved with identical coherence, either up or down; subjects were cued to attend one of the patches and discriminate its direction of motion with a button press. Brain responses and behavior were measured for six different levels of motion coherence (from 0%, or wholly random, to 100%, corresponding to fully coherent motion of the entire patch of dots; Fig. 1b), and for static control trials in which the dots did not move. Each trial was presented in rapid succession using an event-related design¹⁵. The relationship between BOLD contrast and stimulus coherence was characterized throughout the brain without using any *a priori* assumptions about either the form of that relationship or the location of activated areas.

Behavioral

Psychometric functions derived from subject responses during scanning were fit with Weibull functions (Fig. 1c). The mean coherence threshold (75% correct, two-alternative forced choice) was 31.6% (s.e.m., 8%). This is comparable to thresholds measured for human observers at similar retinal eccentricities¹⁶ but greater than reported for foveal presentation in monkey⁴, presumably due to the eccentricity.

Functional imaging

Polynomial regression (Methods) was used to estimate the brain responses to individual trials at each level of stimulus coherence¹⁷. This technique allows the determination of any relationship between stimulus coherence and brain responses that is well fit by a polynomial function (Methods and Fig. 2). Each component of this statistical model was sequentially tested to see if it accounted for a significant proportion of the variance, independent of the other components.

The first-order term modeled a linear relationship between brain responses and stimulus coherence, after the constant term (of no experimental interest) had been taken into account. Several different brain areas in extrastriate cortex showed a significant first-order (linear) component to the relationship between their

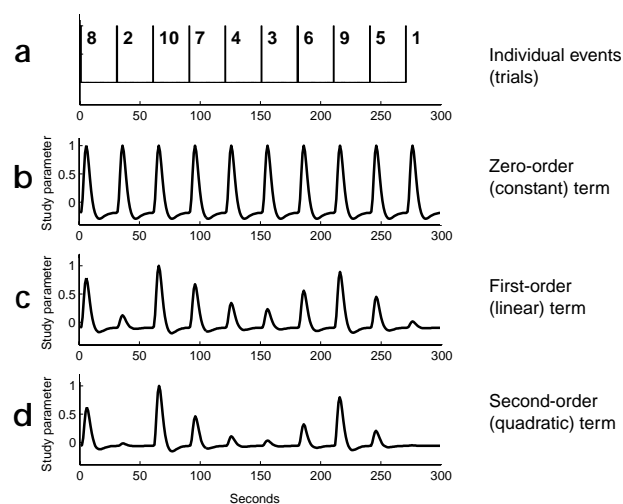


Fig. 2. Polynomial expansion, introduced in terms of the hemodynamic response function typically used in event-related fMRI. (a) Times of occurrence of ten individual trials, each representing a different level of a stimulus parameter (numbers to the right of the trial onset). In the experiment, these values were the stimulus coherence. (b–d) Individual trials convolved with a hemodynamic response function to create typical event-related regressors. (c and d) First-order (c) and second-order (d) terms. These are the element-wise products of a linear (or quadratic) term derived from the parameter values in (a) and the hemodynamic response function. Each regressor is normalized to an arbitrary maximum value. Multiple linear regression of regressors B, C and D on the fMRI time series establishes the degree to which each contributes to the overall response (Methods). In the actual experiment, the inter-trial interval was much shorter and each regressor was orthogonalized with respect to the lower-order terms.

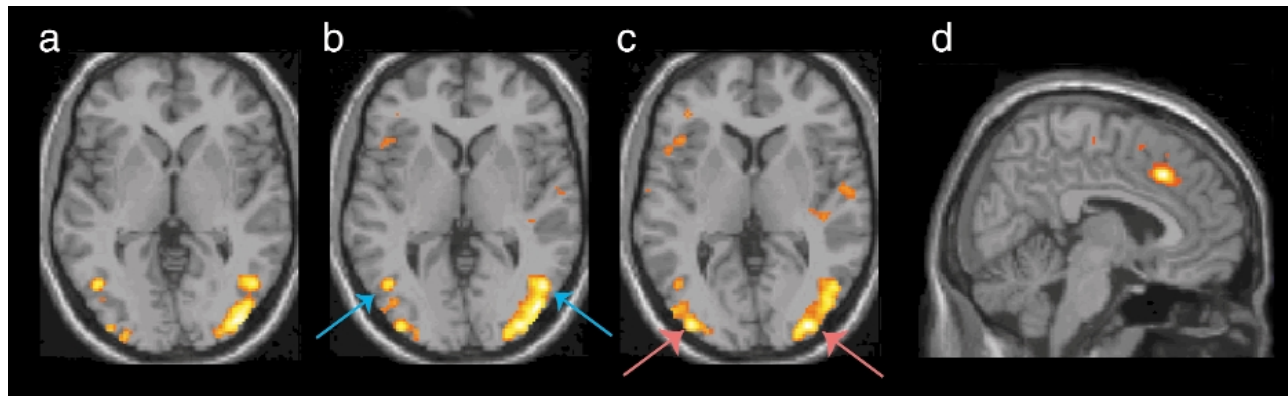


Fig. 3. Brain areas showing a linear relationship with stimulus coherence. (a–c) Three contiguous slices at Talairach coordinates $z = -2$, $z = 0$ and $z = 2$ show loci (Table 1) at which brain activity (averaged across all four subjects) had a positive linear relationship with stimulus coherence. Activations are overlaid on a canonical T1 anatomical image to aid visualization. Blue arrows, loci corresponding to the stereotactic location of human V5 (ref. 18); red arrows, loci corresponding to the stereotactic location of human KO²⁴. (d) Activation in the anterior cingulate gyrus showing a negative linear relationship with stimulus coherence (Table 1), overlaid on a sagittal slice of the same canonical T1 anatomical image.

BOLD responses and stimulus coherence (Table 1 and Fig. 3). The most anterior of the extrastriate areas were in bilaterally homologous positions consistent with human V5 complex^{8,9,18}. Posterior to the V5 complex, bilateral foci of activation were identified in locations consistent with the 'kinetic occipital' (KO) area¹⁹. Weaker and less-reliable activations were observed in bilaterally symmetric inferior areas consistent with V2, and a number of other small foci in extrastriate cortex (Table 1). The weaker motion selectivity of these areas agrees with previous observations⁹. All of these loci were positively weighted on the linear term, indicating a significant linear increase in activity as stimulus coherence increased. The calcarine sulcus was specifically inspected, but did not show modulation of activity with stimulus coherence.

Two areas in frontal cortex, anterior cingulate gyrus (Fig. 3d) and left insula (Table 1), showed a significant linear relationship between BOLD contrast and stimulus coherence. The absolute magnitude of these changes and their statistical significance were larger than those in extrastriate cortex (Table 1). However, unlike extrastriate cortex, in these frontal areas the weighting of the first-order term was negative, indicating that BOLD contrast decreased as stimulus coherence increased (Fig. 4c).

The second-order term modeled a quadratic (nonlinear) relationship between brain responses and stimulus coherence, after lower-order terms had been taken into account. Adding this term improved the overall fit of our statistical model in only a very restricted set of areas (Table 1). In area V5, there was no significant improvement in fit for any voxel, even at very low ($p < 0.01$, uncorrected) statistical thresholds (Fig. 4a). Significant

improvements in fit (all positively accelerating nonlinearities) were observed only in three isolated areas located approximately 30 mm posterior and slightly superior to area V5 (Table 1). Two loci were bilaterally symmetric located immediately posterior and superior to the loci previously identified as 'KO' with the first-order fit. The third area, located still more superiorly and posteriorly, was in a location consistent with human V3a (ref. 20). In frontal cortex, addition of a second-order term led to a weak improvement in the statistical fit of the model in anterior cingulate cortex ($x, y, z = \{6\ 22\ 40\}$, $F = 9.46$, $p = 0.002$ uncorrected; Fig. 3).

Table 1. Stereotactic coordinates and F statistics for brain areas in which a first- or second-order relationship with stimulus coherence accounted for a significant proportion of the variance.

| Cortical area | Talairach coordinates | | | F statistic |
|-------------------------------|-----------------------|------|-----|---------------|
| | X | Y | Z | |
| First-order, positive | | | | |
| Right V5 | 50 | -66 | 0 | 29.30 |
| Left V5 | -44 | -64 | -2 | 23.93 |
| Right KO | 40 | -86 | -2 | 30.33 |
| Left KO | -36 | -90 | 2 | 27.24 |
| Right V2 | 20 | -90 | -20 | 19.24 |
| Left V2 | -16 | -90 | -18 | 13.45 |
| Right fusiform | 22 | -68 | -10 | 19.57 |
| Left occipital gyrus | -26 | -94 | 16 | 10.95 |
| Left middle occipital gyrus | -36 | -82 | 14 | 20.05 |
| First-order, negative | | | | |
| Right anterior cingulate | 6 | 24 | 40 | 48.28 |
| Left insula | -52 | 14 | 8 | 31.97 |
| Second-order, positive | | | | |
| Right middle occipital gyrus | 28 | -94 | 6 | 21.39 |
| Left middle occipital gyrus | -32 | -92 | 4 | 13.93 |
| Right V3a | 12 | -100 | 4 | 18.19 |

Data represent loci where BOLD contrast showed a positive first-order (linear) relationship with stimulus coherence, a negative linear relationship with coherence or a positive second-order (nonlinear) relationship with stimulus coherence. Only the most significant peak within each area of activation is reported. A statistical threshold of $p < 0.001$, uncorrected for multiple comparisons, was used within extrastriate cortex. Elsewhere, a correction for multiple comparisons was made at a threshold of $p < 0.05$, corrected.

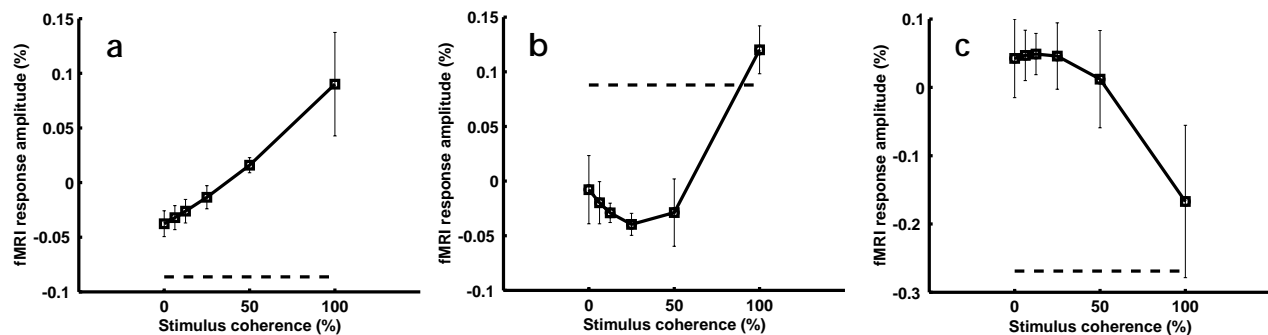


Fig. 4. fMRI responses to stimulus coherence in three representative cortical areas. (a) Brain responses in human V5 plotted as a function of stimulus coherence. Data represent the modulation of brain responses accounted for by first- and second-order terms around the mean response established by the zero-order (constant) term. This is equivalent to normalizing the responses to an overall mean of zero. Data are averaged between left and right hemispheres and across subjects (Table 1, coordinates; Methods, details of averaging). Error bars, one standard deviation of the inter-subject variability. Dotted line, equivalent BOLD response to the null trials, in which a fixed display is flashed onto the screen with no motion. These null trials are normalized to the mean activity established by the constant term, in the same way as the responses to trials in which the stimulus contained motion. (b) Brain responses from loci showing a significant improvement with the addition of a second-order (nonlinear) term that are posterior to V5 (Table 1), plotted as a function of stimulus coherence. Dotted line, response to null trials in which no motion was present. (c) Brain responses from the anterior cingulate, plotted using the same conventions as in a and b.

The third-order term modeled a higher-order nonlinear relationship between brain responses and stimulus coherence, after lower-order terms had been taken into account. Adding a third-order term to the model did not significantly improve the overall statistical fit of the model in any brain areas. Therefore, no terms higher than third-order were tested.

Detailed characterization of fMRI responses

Three regions were selected for further characterization: anterior cingulate, area V5 and the posterior extrastriate regions that showed a significant improvement in fit with addition of a quadratic (nonlinear) term. For each area, BOLD responses were determined as a function of stimulus coherence (Fig. 4), after removal of the zero-order term (equivalent to mean-correcting the data). As right and left motion-sensitive areas did not differ significantly in their activation, homologous regions were averaged between hemispheres. This provided a measure of the percentage change in BOLD contrast from the mean activity (over all coherence levels, but not including null trials) in each cortical area as a function of stimulus coherence. To avoid biasing our estimation of these evoked responses by selecting data from only a single voxel, the average responses were computed for a sphere of radius 3 mm centered on the voxel of peak activation. Qualitatively, changing the radius of this sphere (3–9 mm) did not alter the pattern of the results.

Null (no motion) trials

For one-third of the trials, the dots were flashed and then remained static throughout the 250-ms trial. Subjects were instructed to respond with a single button press to such null trials, and subsequent evaluation of their responses confirmed that they were equally likely to press either button on such trials. The inclusion of such trials was motivated by earlier reports that human area V5 responds strongly to flicker⁹. Although sudden onsets and offsets of static displays contain no 'movement' themselves, they evoke motion energy that could activate detectors sensitive to motion energy, and indeed stimulus onsets and offsets produce sizeable activation of V5 in monkey^{21,22}. To assess the size of such transient responses relative to the activation produced by the coherently moving stimuli, we calculated the over-

all level of activation produced by null trials relative to the mean level of activation in extrastriate areas (Fig. 4, horizontal dashed lines). The mean level of activation produced by null trials was comparable to that produced by zero percent coherence trials in V5 (Fig. 4a), and exceeded that of coherent trials in the more posterior extrastriate areas (Fig. 4b).

Reproducibility of fMRI findings

The preceding analyses were based on a fixed-effects model within four subjects²³. Individual response profiles were also determined to assess intersubject variability (Fig. 5). There was excellent agreement in the form of the response profiles across all four subjects. For area V5, although subjects showed slight nonlinearities in the relationship between BOLD contrast and stimulus coherence, these were not significant ($p < 0.001$, uncorrected) and were equally likely to be positively or negatively accelerating (Fig. 5). All subjects showed nonlinear U-shaped responses in the more posterior extrastriate brain areas; similar reproducibility was evident for the anterior cingulate activation (data not shown).

Summary of fMRI results

These data demonstrate that a remarkably restricted set of cortical areas show covariation of BOLD responses with the strength of stochastic motion signals. The strongest covariation was observed in extrastriate motion-sensitive areas V5 (ref. 8), KO²⁴ and V3a (ref. 20) and in the anterior cingulate gyrus. Among these cortical areas, V5 was distinguished by a strong and strikingly linear positive correlation between BOLD contrast and stimulus coherence, whereas other cortical areas showed either a negative relationship or nonlinear U-shaped responses. We will focus on the quantitative relationship between BOLD responses in human V5 and single-neuron activity in monkey V5 before discussing differences in response properties comparing V5 and other cortical areas.

DISCUSSION

Relating single-neuron responses to fMRI

Single V5 neurons in macaque also show responses correlated with motion coherence in their preferred direction. Responses

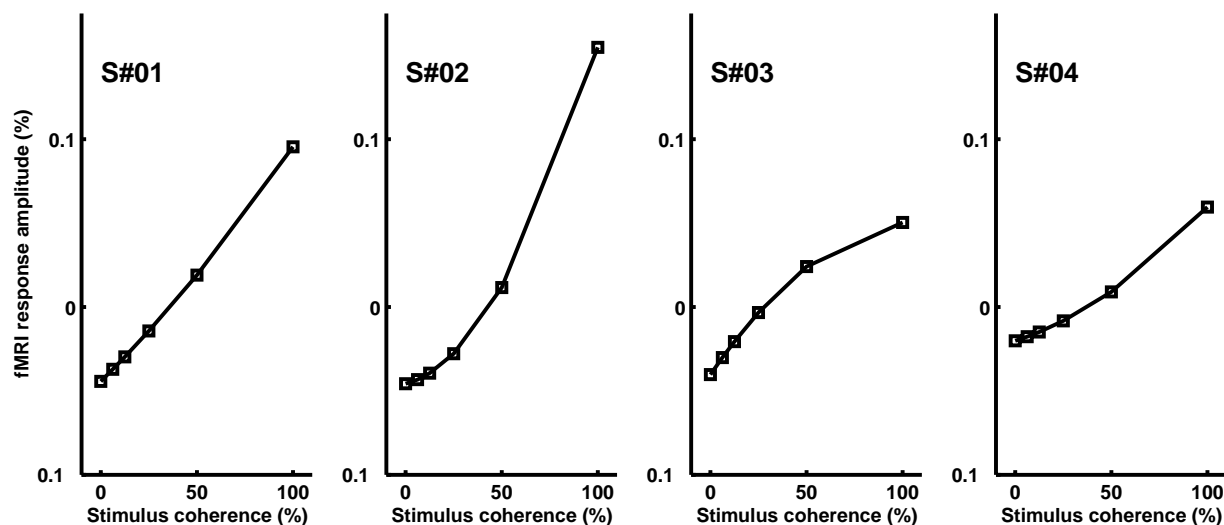


Fig. 5. Reliability of responses across subjects in V5. Brain responses for each individual subject in V5 (Fig. 3b and Table 1), plotted as a function of stimulus coherence. Data were obtained in the same way as in Fig. 4a, but are plotted separately for each subject. The similarity between subjects is evident. Any nonlinear (quadratic) component to these responses was equally likely to be positive or negative, and did not significantly improve the fit compared with a linear component alone.

of cells in area V5 of the awake macaque increase monotonically with coherence in their preferred direction, and decrease with increasing coherence in the null direction⁷. For most cells, their response is best described by a linear function of stimulus coherence. Specifically, for 114 of 216 cells in this study⁷, a quadratic fit to the firing rate as a function of coherence either does not improve the linear fit at all (76 of 216) or improves it only modestly (38 of 216). For the remaining 102 neurons, a quadratic term improves the fit significantly. However, quadratic contributions are small (median value of r^2 increasing by 5.8%), and as likely to be positive as negative.

At a qualitative level, there are therefore strong similarities between BOLD responses in human V5 that reflect neuronal populations, and single-cell responses in macaque V5. However, as previously noted¹², an apparent qualitative similarity between single-neuron and population responses may be misleading, and we therefore undertook a quantitative mathematical exploration of this relationship. Anatomically, the direction selectivity of cells within V5 is topographically mapped so that 180 degrees of axis of motion are represented in 400–500 μm of cortex²⁵. Physiological and psychophysical data in monkey and human shows an isotropic distribution of direction preferences^{26,27}, so within each fMRI voxel it is reasonable to assume that all direction preferences are equally represented. Thus, expected neuronal activity A (in spikes/second) is given by integrating over the activity of neurons of all direction preferences:

$$A = \int_0^{2\pi} f(c, \theta, \theta_p) \cdot p(\theta_p) d\theta_p$$

$$\text{where } \int_0^{2\pi} p(\theta_p) d\theta_p = 1 \quad (1)$$

Here, $f(c, \theta)$ is the response of a neuron (in spikes per second per unit) to a stimulus with coherence c and direction θ , where that neuron has a preferred direction θ_p . $p(\theta_p)$ is the probability that any neuron selected at random from the voxel has preference θ_p . As the voxel subsumes all directional selectivities, the latter prob-

ability can be assumed to be constant: $p(\theta_p) = 1/(2\pi)$. The response of any neuron can now be decomposed into the activity α at a stimulus coherence level of zero percent and its response to increasingly coherent motion in the preferred and null directions:

$$f(c, \theta, \theta_p) = \alpha + g_p(c)h(\theta_p - \theta) + g_N(c)h(\theta_p + \pi - \theta)$$

$$\text{where } h(\theta) = \exp(-\theta^2 / 2\sigma^2) \quad (2)$$

Here, the 'receptive field' of the neuron has been factored into functions of coherence and direction for both preferred and null directions, consistent with physiological evidence for separability²⁸. The function h embodies the direction selectivity of the neuron and can be thought of as a tuning curve with width σ . For convenience, the tuning curves are modelled as Gaussians, but this assumption is not critical for our conclusions. Empirically, the previous single-neuron data⁷ demonstrate that a first-order approximation to $g_p(c)$ and $g_N(c)$ is sufficient to account for observed responses where

$$g_p(c) = \beta c \text{ and } g_N(c) = \gamma c \quad (3)$$

Empirical estimates of β and γ were obtained⁷ by presenting stimuli of different coherences in the preferred and null directions where $h(\theta_p - \theta) = 1$ and $h(\theta_p + \pi - \theta) = 0$ and *vice versa*. Across the entire neuronal population in macaque V5 examined⁷, the average values of β and γ (the slopes of the coherence response function in preferred and null directions) are 0.4 spikes per percent coherence per second and -0.1 spikes per percent coherence per second, respectively (K.H. Britten, personal communication). Substituting Equation 2 and Equation 3 into Equation 1, leads to

$$A = \alpha + c(\beta + \gamma)\sigma/\sqrt{2\pi} \quad (4)$$

This equation suggests that the population spiking rate of macaque V5 will rise linearly as coherence increases. Our find-

ings in human V5 of a similar linear relationship between BOLD responses and stimulus coherence therefore imply a proportional relationship between population spiking rate and BOLD signal. Thus, for BOLD signal B we have

$$B = \phi A \Rightarrow \phi = \frac{\delta B}{\delta c} \times \frac{\sqrt{2\pi}}{\sigma(\beta + \gamma)} \quad (5)$$

where ϕ , the constant of proportionality, is the BOLD signal per spike per second per unit. We can estimate this constant for any tuning curve width. For example, given our regression slope estimate from Fig. 4a of 0.005185 (percent BOLD/percent coherence corrected for a stimulus duration of 250 ms) and assuming that $\sigma = \pi/8$ (that is, a tuning curve FWHM of $\sim 53^\circ$), then the constant of proportionality, ϕ , represented in Equation 5 is 0.1103. In other words, each percent increase in BOLD signal represents a mean increase of about 9 spikes per second per unit ($1/0.1103 \approx 9$), in the functionally responsive population within the voxel.

This simple quantitative mathematical relationship relies on only three assumptions, all of which are supported by direct physiological evidence: homogenous distribution of neuronal directional preferences²⁵, and Gaussian directional tuning that does not change as a function of stimulus coherence²⁸ (separability). Furthermore, our estimate of ϕ depends on just four parameters: the slopes of the coherence response functions from single-neuron recordings and fMRI, and the width of the tuning curve. Precise estimates of the variability in each parameter are difficult to establish, but if we assume a proportionate error of up to 30% in our estimate of each parameter, then Gaussian error propagation suggests that the overall error in our estimate of ϕ is within a range of 4.5–14 spikes per second per percent BOLD contrast (in a 2.0T scanner). Thus our estimate of ϕ is both relatively robust and within a physiologically plausible range. Empirical findings from different experimental techniques in different species are therefore linked by a simple linear relationship, allowing an explicit quantitative connection to be made between single-neuron activity and BOLD population responses in human and monkey V5.

Relating fMRI to computational models of single neurons

Computational models of both motion detection²⁹ and single V5 neurons have been proposed³⁰. The current single-cell models are composed of physiologically plausible components and accurately reproduce observations made in single-cell electrophysiology experiments³⁰. Our finding of a simple proportional relationship between aggregate single-neuron and fMRI population activity represents a mathematical relationship that is independent of the specific neuronal mechanism that generates the selective properties of individual V5 cells. However, inasmuch as the currently accepted model³⁰ accurately reproduces the single-cell data from which we have derived the mathematical relationship between single-neuron and fMRI activity, our results are consistent with such a model.

On theoretical grounds, it has been suggested that the relationship between neuronal population activity and functional imaging measures may be complex. Considering a neuronal population, stimulus changes that result in response modulation of a small number of neurons might be exactly balanced by increased baseline firing of a larger number of other neurons¹². Thus although individual neurons may show strong changes in firing rates, overall population activity could remain unchanged if it were exactly balanced by a small increase in baseline firing across the population. Our empirical observation of a strong dependence of fMRI signal on stimulus coherence shows that this is not true for human V5. At the level of single neurons, our find-

ings therefore suggest that changes in response modulation due to stimulus coherence are not exactly balanced by changes in baseline firing, consistent with recent physiological data in macaque²⁸.

Comparing responses in V5 and other motion-sensitive areas

We found striking and previously unknown dissociations in response profiles comparing V5 and other motion-sensitive areas. The responses of homologous areas in macaque have not been explored. However, the simple linear relationship we demonstrated between BOLD responses in human V5 and single neurons in macaque V5 suggests that a similar relationship will hold for these other areas. Our data therefore make clear predictions for the response properties of single cells in homologous areas of macaque cortex, and suggest that the nature of the motion computations performed within these areas is qualitatively different from that in V5.

Our data show a striking anteroposterior dissociation. Although areas of extrastriate cortex showed increased activity with stimulus coherence, two prefrontal areas, the right anterior cingulate and left insula, showed linear decreases in BOLD contrast. This is consistent with one contemporary theory of cingulate function, which suggests that the anterior cingulate is activated in conditions of response conflict under which errors are likely to occur, rather than by errors themselves^{31,32}. Neurons in V5 are strongly direction selective^{1,26,27}, and as coherence is reduced from 100%, the proportion of dots moving in different directions increases. Our subjects were asked to make a motion discrimination, so if each V5 neuron contributes to the decision-making process, increasing competition would occur from different direction-selective neurons responding to the mix of different directions of motion as display coherence decreases. At high coherence, only a single population of direction-selective neurons responds strongly, leading to decreased response competition. Such a qualitative explanation seems able to account for our observations in prefrontal cortex, but further study of cingulate involvement in this task may prove useful.

A further dissociation in response profiles was found between V5 and more posterior areas. Adding a second-order (quadratic) term to the model did not improve the overall fit in human V5 (Fig. 3a). However, three areas located some 25 mm posterior to V5 showed highly significant nonlinearities, with a U-shaped response profile and a prominent minimum at 50% coherence (Fig. 3b). Two of these loci were located just posterior and abutting on the coordinates previously described for KO. At these coordinates, the response profile showed only a statistical trend toward improvement of the model fit with inclusion of a nonlinear term. Further investigation will be needed to clarify whether these regions of nonlinear responses to stimulus coherence are distinct from area KO, or represent a functional subdivision of this area. The third locus that showed a significant nonlinear response profile was located slightly superior and medial to the other loci in a position corresponding to human V3a (refs. 20,33). The homology between KO in humans and the equivalent area in monkey is unknown at present, so the response properties of single cells are not available for comparison. However, the clear dissociation in response profiles between all of these motion-sensitive loci and area V5 shows clearly that the nature of the computation taking place in these areas in response to moving stimuli must be different.

Conclusion

Our analysis indicates that a very simple mathematical expression links changes in the stimulus coherence, changes in single-neuron

firing rates in awake monkeys and modulation of BOLD contrast in humans. These findings suggest that BOLD contrast is directly proportional to the average neuronal firing rate, consistent with recent suggestions¹³, and indicate strong functional homology between human V5 and macaque MT. Moreover, our results provide a quantitative estimate of the constant of proportionality between BOLD population responses in humans and single-neuron responses in the awake monkey. Our data suggest a constant of approximately 9 spikes per second per unit per percent BOLD contrast in the functionally responsive population in human V5. Such an estimate seems not unreasonable, but clearly depends on a number of simplifying assumptions about the metabolic equivalence of macaque and human neocortex, relative proportion of excitatory and inhibitory cells, and many other factors. Nevertheless, these data emphasize the power of quantitative parametric neuroimaging studies. It will be of considerable interest to see how such estimates compare with measurements of BOLD contrast and spiking activity simultaneously using fMRI in awake, behaving monkeys¹¹.

METHODS

Subjects. Four subjects with normal or corrected-to-normal vision (mean age, 28 years; range, 25–32 years) gave informed consent. One was an experienced psychophysical observer and three were naive; all were shown the stimuli and task beforehand to ensure that they understood the task requirements.

Visual stimuli. Single trials were presented for 250 ms, using an Liquid Crystal Display (LCD) projector and a small mirror mounted above the subject's head. For each trial, two stochastic motion stimuli were presented within circular apertures of radius two degrees centered four degrees symmetrically to the left and right of a small fixation cross. Each aperture contained 20 dots per degree², each subtending ~2 arc min, which moved on each frame at a velocity of ~5 degrees per s. Dots were white, of 100% contrast on a black background. The effective frame rate (limited by the LCD projector) was 60 Hz. The proportion of dots chosen anew on each frame defined the coherence of the display, and moved vertically either up or down. Dots that did not move coherently were randomly replotted on each frame. In the terminology of Scase³⁴, these displays used the 'same different' rules used before in ref. 5 and by others. Each trial lasted 250 ms and was preceded for 500 ms by a small pre-cue symbol presented at central fixation, indicating the aperture that the subject was required to attend and report on the upcoming trial. Although the coherence of the stimuli presented in each aperture were identical, direction was randomized so subjects were required to attend to the cue aperture to report correctly. Subjects were expressly required to maintain fixation at all times, and adequacy of fixation was ensured by direct monitoring outside the scanner before and after the experiment. Following each trial, subjects indicated their report of motion direction by pressing one of two buttons with their dominant hand. Both speed and accuracy were emphasized.

For one-third of the trials, the stimuli were presented in exactly the same way, but the individual dots remained static throughout the trial duration. Subjects were asked to respond with a single button press. These 'null trials' were included to assess the response of motion-sensitive areas to flashed stimulus onsets, and were matched in all respects to the experimental trials with the exception of the absence of moving dots.

Trials were presented in a steady continuous stream with a stimulus onset asynchrony of 2.1 s. Presentation order was determined pseudo-randomly by a transition matrix that determined the transition probabilities between trials of different levels of coherence and direction of attention independently. This ensured that pairs or triplets of trials sharing similar characteristics occurred together more frequently than would obtain by chance. This manipulation improves the power of an event-related design with multiple experimental conditions, compared with that of a fully randomized design¹⁵. Informal debriefing of the subjects confirmed that none detected this experimental manipulation.

During the experiment, 576 trials in total were presented per subject, divided between four imaging runs. Of these, one-third (192) were null trials, whereas the remainder were divided equally between six different coherences (0, 6.25%, 12.5%, 25%, 50% and 100%) and direction of the pre-cue (left–right). This experiment therefore represents a parametric factorial event-related design, in which two factors are independently manipulated: the degree of coherence of the motion displays, and the direction of attention to either right or left aperture. In this report, we considered only the effects of coherence on the BOLD response, leaving an analysis of attentional modulation for the future.

Functional imaging. A 2T VISION scanner (Siemens, Erlangen, Germany) acquired BOLD image volumes, of 32 contiguous 3-mm slices with an in-plane resolution of 3 × 3 mm and repetition time of 2,800 ms. Scanning took place in four runs of 164 volumes. The first six scans of each run were discarded to allow for T1 equilibration effects. A T1-weighted anatomical image was acquired at the beginning of the session.

Data preprocessing. SPM99 (Wellcome Department of Cognitive Neurology, London: <http://www.fil.ion.ucl.ac.uk/spm>) was used for fMRI data preprocessing and statistical analysis. Each image volume was realigned to the first volume, spatially normalized to the space of Talairach & Tournoux³⁵ with subsampling to a resultant voxel size of 2 × 2 × 2. The resultant image volumes were spatially smoothed with a Gaussian kernel of 8 mm full-width half-maximum before statistical analysis^{36,37}.

Statistical analysis. Functional imaging data analysis typically uses linear regression (or cross-correlation) between the observed signal and a regressor to identify different patterns of activation in the data³⁸. Here we sought to identify the form of the relationship between the experimental parameter (coherence) and hemodynamic responses. However, the nature of this response was unknown in advance and may vary in different brain regions. Therefore, an *a priori* definition of a fit function for a standard linear regression analysis may result in a partial and misleading characterization of the data. We therefore adopted an approach, polynomial regression, that embodied no such prior assumptions to characterize our data. This extension to standard analytic techniques is described fully elsewhere with respect to conventional blocked designs^{17,39}, but we applied it here for the first time to an event-related design.

We characterized brain responses as a linear combination of basis functions of the experimental parameter (coherence), thus

$$y = \alpha + \beta_1 c + \beta_2 c^2 + \dots + \beta_n c^n + \varepsilon$$

Here, α represents the constant term; c , the stimulus coherence; and ε , the residual error after each component of the polynomial expansion has been fitted to the data. Using nonlinear functions of the task parameter allows nonlinear responses to be modeled within the context of the general linear model. This approach was extended to the analysis of the fMRI time series by creating time-varying regressors that reflected the expected brain response for each term in the polynomial expansion of stimulus coherence (Fig. 2). Specifically, we created regressors that represented the interaction between stimulus coherence c and a train of delta functions representing the individual experimental trials convolved with a canonical hemodynamic response function. The different terms were orthogonalized serially with respect to the lower-order terms as described¹⁷.

Each of the regressors represents one component of the expected brain response to stimulus coherence. Thus, some linear combination of the regressors can model any brain response that is well fit by such a polynomial expansion. Different sets of regressors modeled the expected response to cued (variable stimulus coherence) and null (no motion) trials, each serving as a regressor in a multiple regression analysis at each voxel. Before regression, high-pass filtering removed low-frequency drifts in signal, and global changes in activity were removed by proportional scaling. As each slice in the image volume was acquired asynchronously in a descending manner, a constant offset was applied to each event train to optimize sensitivity in visual cortex. The resultant parameter estimates

for each regressor at each voxel were compared using *F*-tests to determine whether significant activation due to each component had occurred. To assess the fit of each of the polynomial regressor components separately, a serial forward hierarchical analysis was performed. Starting with the 'zeroth-order' components, progressively higher-order components were added to the regression until no significant improvement in the overall fit (as assessed by *F*-tests) occurred⁴⁰.

Statistical results given are based on a single-voxel *F* threshold of 10.91 (corresponding to $p < 0.001$, uncorrected for multiple comparisons), unless otherwise stated. We made no further correction for multiple comparisons within striate and extrastriate areas, for which we had *a priori* hypotheses. Outside these areas, a correction was made for multiple comparisons across the whole brain volume, as we had no prior hypothesis for non-visual areas.

ACKNOWLEDGEMENTS

This work was supported by the Wellcome Trust, the Keck Foundation, the National Science Foundation and the National Institutes of Mental Health. We thank K.H. Britten for comments on the manuscript.

RECEIVED FEBRUARY 23; ACCEPTED MAY 9, 2000

- Zeki, S. M. Functional organization of a visual area in the posterior bank of the superior temporal sulcus of the rhesus monkey. *J. Physiol. (Lond.)* **236**, 549–573 (1974).
- Allman, J. M. & Kaas, J. H. A crescent-shaped cortical visual area surrounding the middle temporal area (MT) in the owl monkey (*Aotus trivirgatus*). *Brain Res.* **81**, 199–213 (1974).
- Parker, A. J. & Newsome, W. T. Sense and the single neuron: probing the physiology of perception. *Annu. Rev. Neurosci.* **21**, 227–277 (1998).
- Britten, K. H., Shadlen, M. N., Newsome, W. T. & Movshon, J. A. The analysis of visual motion: a comparison of neuronal and psychophysical performance. *J. Neurosci.* **12**, 4745–4765 (1992).
- Newsome, W. T. & Pare, E. B. A selective impairment of motion perception following lesions of the middle temporal visual area (MT). *J. Neurosci.* **8**, 2201–2211 (1988).
- Salzman, C. D., Britten, K. H. & Newsome, W. T. Cortical microstimulation influences perceptual judgements of motion direction. *Nature* **346**, 174–177 (1990).
- Britten, K. H., Shadlen, M. N., Newsome, W. T. & Movshon, J. A. Responses of neurons in macaque MT to stochastic motion signals. *Vis. Neurosci.* **10**, 1157–1169 (1993).
- Zeki, S. *et al.* A direct demonstration of functional specialization in human visual cortex. *J. Neurosci.* **11**, 641–649 (1991).
- Tootell, R. B. *et al.* Functional analysis of human MT and related visual cortical areas using magnetic resonance imaging. *J. Neurosci.* **15**, 3215–3230 (1995).
- Kwong, K. K. *et al.* Dynamic magnetic resonance imaging of human brain activity during primary sensory stimulation. *Proc. Natl. Acad. Sci. USA* **89**, 5675–5679 (1992).
- Logothetis, N. K., Guggenberger, H., Peled, S. & Pauls, J. Functional imaging of the monkey brain. *Nat. Neurosci.* **2**, 555–562 (1999).
- Scannell, J. W., Young, M. P. Neuronal population activity and functional imaging. *Proc. R. Soc. Lond. Biol. Sci.* **266**(1422), 875–881 (1999).
- Heeger, D. J., Boynton, G. M., Demb, J. B., Seidemann, E. & Newsome, W. T. Motion opponency in visual cortex. *J. Neurosci.* **19**, 7162–7174 (1999).
- Wandell, B. A. Computational neuroimaging of human visual cortex. *Annu. Rev. Neurosci.* **22**, 145–173 (1999).
- Josephs, O. & Henson, R. N. Event-related functional magnetic resonance imaging: modelling, inference and optimization. *Phil. Trans. R. Soc. Lond. B Biol. Sci.* **354**, 1215–1228 (1999).
- Raymond, J. E. Directional anisotropy of motion sensitivity across the visual field. *Vision Res.* **34**, 1029–1037 (1994).
- Buchel, C., Wise, R. J., Mummary, C. J., Poline, J. B. & Friston, K. J. Nonlinear regression in parametric activation studies. *Neuroimage* **4**, 60–66 (1996).
- Watson, J. D. *et al.* Area V5 of the human brain: evidence from a combined study using positron emission tomography and magnetic resonance imaging. *Cereb. Cortex* **3**, 79–94 (1993).
- Van Oostende, S., Snaets, S., Van Hecke, P., Marchal, G. & Orban, G. A. The kinetic occipital (KO) region in man: an fMRI study. *Cereb. Cortex* **7**, 690–701 (1997).
- DeYoe, E. A. *et al.* Mapping striate and extrastriate visual areas in human cerebral cortex. *Proc. Natl. Acad. Sci. USA* **93**, 2382–2386 (1996).
- Zeki, S. The response properties of cells in the middle temporal area (area MT) of owl monkey visual cortex. *Proc. R. Soc. Lond. B Biol. Sci.* **207**, 239–248 (1980).
- Malonek, D., Tootell, R. B. & Grinvald, A. Optical imaging reveals the functional architecture of neurons processing shape and motion in owl monkey area MT. *Proc. R. Soc. Lond. B Biol. Sci.* **258**, 109–119 (1994).
- Friston, K. J., Holmes, A. P. & Worsley, K. J. How many subjects constitute a study? *Neuroimage* **10**, 1–5 (1999).
- Dupont, P. *et al.* The kinetic occipital region in human visual cortex. *Cereb. Cortex* **7**, 283–292 (1997).
- Albright, T. D., Desimone, R. & Gross, C. G. Columnar organization of directionally selective cells in visual area MT of the macaque. *J. Neurophysiol.* **51**, 16–31 (1984).
- Maunsell, J. H. & Van Essen, D. C. Functional properties of neurons in middle temporal visual area of the macaque monkey. I. Selectivity for stimulus direction, speed, and orientation. *J. Neurophysiol.* **49**, 1127–1147 (1983).
- Albright, T. D. Direction and orientation selectivity of neurons in visual area MT of the macaque. *J. Neurophysiol.* **52**, 1106–1130 (1984).
- Britten, K. H. & Newsome, W. T. Tuning bandwidths for near-threshold stimuli in area MT. *J. Neurophysiol.* **80**, 762–770 (1998).
- Adelson, E. H. & Bergen, J. R. Spatiotemporal energy models for the perception of motion. *J. Opt. Soc. Am. [A]* **2**, 284–299 (1985).
- Simoncelli, E. P. & Heeger, D. J. A model of neuronal responses in visual area MT. *Vision Res.* **38**, 743–761 (1998).
- Carter, C. S. *et al.* Anterior cingulate cortex, error detection, and the online monitoring of performance. *Science* **280**, 747–749 (1998).
- Devinsky, O., Morrell, M. J. & Vogt, B. A. Contributions of anterior cingulate cortex to behaviour. *Brain* **118**, 279–306 (1995).
- Tootell, R. B. *et al.* Functional analysis of V3A and related areas in human visual cortex. *J. Neurosci.* **17**, 7060–7078 (1997).
- Scase, M. O., Braddick, O. J. & Raymond, J. E. What is noise for the motion system? *Vision Res.* **36**, 2579–2586 (1996).
- Talairach, J. & Tournoux, P. *Co-Planar Stereotaxic Atlas of the Human Brain* (Georg Thieme Verlag, New York, 1988).
- Friston, K. J. *et al.* Spatial realignment and normalisation of images. *Hum. Brain Mapp.* **2**, 165–189 (1995).
- Turner, R., Howseman, A., Rees, G. E., Josephs, O. & Friston, K. Functional magnetic resonance imaging of the human brain: data acquisition and analysis. *Exp. Brain Res.* **123**, 5–12 (1998).
- Friston, K. J. *et al.* Statistical parametric mapping in functional imaging: a general linear approach. *Hum. Brain Mapp.* **2**, 189–210 (1995).
- Buchel, C., Holmes, A. P., Rees, G. & Friston, K. J. Characterizing stimulus-response functions using nonlinear regressors in parametric fMRI experiments. *Neuroimage* **8**, 140–149 (1998).
- Draper, N. R. & Smith, H. *Applied Regression Analysis* (Wiley, New York, 1981).